Identification of RNA-binding sites in artemin based on docking energy landscapes and molecular dynamics simulation

Behnam Rasti[1], Seyedeh Shirin Shahangian[1], Majid Taghdir[*1], Sadegh Hasannia[1], Reza Hasan Sajedi[2]

[1]Department of Biology, Faculty of Science, University of Guilan, P.O. Box 41335-1914, Rasht, I.R. Iran
[2]Department of Biochemistry, Faculty of Biological Sciences, Tarbiat Modares University, P.O. Box 14115-111, Tehran, I.R. Iran

Abstract
There are questions concerning the functions of artemin, an abundant stress protein found in *Artemia* during embryo development. It has been reported that artemin binds RNA at high temperatures *in vitro*, suggesting an RNA protective role. In this study, we investigated the possibility of the presence of RNA-binding sites and their structural properties in artemin, using docking energy landscapes and molecular dynamics simulation. Analysis of docking energy landscapes revealed sites in artemin with the potential of binding RNAs. We found a good agreement between RNA-binding sites of artemin and RNA-interacting sites of a specific group of RNA-binding proteins called PUF, as regards to the type of their interactions with RNA molecules. Furthermore, the results from molecular dynamics simulation showed that firstly, the presence of RNA molecule and its interaction with artemin cause significant decrease in the secondary structure content of artemin; secondly, RNA-binding sites are mostly located in the low flexible regions. Finally, it seems that these binding sites are distributed in such a way that leads RNA molecule into the interior of the protein, strengthening the previous suggestion for RNA-protecting role of artemin.
Keywords: Artemin; docking energy landscapes; molecular dynamics simulation; RNA-protecting role

INTRODUCTION

Artemin is an abundant stress protein found in *Artemia* and partly responsible for the amazing tolerance of this brine shrimp in harsh environmental conditions such as thermal extremes (Rasti *et al*., 2009; Chen *et al*., 2007; Warner *et al*., 2004; MacRae, 2003; Chen *et al*., 2003; Hontoria *et al*., 1993). As *Artemia* enters diapause stage, artemin appears in the cysts and soon after termination of severe conditions and appearance of larvae, it disappears. It has been previously reported that metabolic dormancy occurs in *Artemia* cysts under diapause conditions and processes such as DNA replication, transcription, translation, mitosis, cytokinesis and cell-division are substantially suppressed during this period (Chen *et al*., 2007; Warner *et al*., 2004; MacRae, 2003; Hontoria *et al*., 1993). There are unanswered questions about the functions of this protein during *Artemia* embryo development. However, it is known that artemin confers stability to transfected mammalian cells against heat and H_2O_2 and inhibits heat-induced aggregation of citrate synthase in vitro (Warner *et al*., 2004; MacRae, 2003). There is also some evidence showing that artemin binds RNA at high temperatures (70ºC) *in vitro*, suggesting a role which is similar to that of RNA-binding proteins (RBPs) that mediate the regulation of gene expression patterns by playing critical roles in transcriptional regulation and post-transcriptional control of RNAs (Warner *et al*., 2004; Johnstone and Lasko, 2001; Curtis *et al*., 1995). Regarding the high tendency of artemin for binding RNAs and its presence during diapause (Warner *et al*., 2004; Hontoria *et al*., 1993), a question that might arise is whether artemin plays a protecting role for RNAs or not. To shed light on this question, we investigated the presence of RNA-bind-

[*]*Correspondence to:* **Majid Taghdir, Ph.D.**
Tel: +98 131 3226643; Fax: +98 131 3220066
E-mail: taghdir@guilan.ac.ir

ing sites in artemin, using the features of RNA-binding sites in RBPs, docking energy landscapes and molecular dynamics simulation.

METHODS

Modeling and structure quality validation: A three-dimensional (3-D) structure model of artemin was constructed using the MODELLER program Ver.9v2 (Sali and Blundell, 1993) based on human ferritin L-chain (pdb code: 2FG4, 48% similarity) (Wang *et al*., 2006) and horse apoferritin L-chain (pdb code: 1AEW, 47% similarity) (Hempstead *et al*., 1997) (http://www.pdb.org/pdb/home/home.do). The Protein Structure Quality Score (PSQS) (Godzik *et al*., 1995; Godzik, 1996; Pawlowski *et al*., 1997; Jaroszewski *et al*., 1998) (http://www1.jcsg.org/psqs), ERRAT (Colovos and Yeates, 1993), Verify3D (Bowie *et al*., 1991) and ProCheck (Laskowski *et al*., 1993) (http://nihserver.mbi.ucla.edu/SAVS) programs were used to validate the quality of the artemin models.
Multiple alignment using a CLUSTAL W (version 1.9; http://www.ebi.ac.uk/clustalw) (Thompson *et al*., 1994) was used for comparative sequence analysis. Secondary structure assignment was carried out using Stride web server (http://webclu.bio.wzw.tum.de/stride/) (Heinig and Frishman, 2004).

Molecular docking: The proposed structural model of artemin and RNA crystal structure (NDB: 1dqf) extracted from Nucleotide Data Bank (NDB) (http://ndbserver.rutgers.edu) (Berman *et al*., 1992) were used for docking. Fourier Transform rigid-body docking package (FTDock) version 2.0 was used to construct docked complexes (Aloy *et al*., 1998). The protein structure was held fixed and the RNA molecule was allowed to move independently. A grid size of 0.7 A°, rotation angle step of 12° and surface thickness of 1.2 A° were employed for docking. The top 10000 docking models ranked by the shape complementarity score (Gabb *et al*., 1997) were obtained. After that, 500 docked structures with the highest shape complementarity score were retained. These models were subsequently energy analyzed and filtered using the energy analysis module of AMBER 9 (Case *et al*., 2000) and the top 100 energy-ranked models were retained for protein-RNA binding energy analysis.

Molecular dynamics (MD) simulation: MD simulations were run for refinement of constructed structures and study of structural changes and internal motions. In MD simulations counter ions (Cl^- and Na^+) were added by replacing water molecules at the most positive/negative electrical potential to achieve a neutral simulation cell. Both initial setup and dynamics runs were carried out by Amber 9. All calculations were performed with a cutoff distance of 10Aº. The protein was solvated with about 6650 molecule of TIP3P model of water (Jorgensen *et al*., 1983) in an octahedron box with a minimum 8Aº distance between the box edge and the closest portion of the molecule. The volumes, total mass and initial density of the box were 281807.158 A^{o3}, 149413.408 amu and 0.88 g/cm^3 respectively. First, the system was energy minimized for 500 steps of steepest descent minimization to remove close Van der Waals contacts and to allow formation of hydrogen bonds between water molecules in the periodic box and the protein. Temperature was increased from 200 to 300 K (and 343 K for high temperature simulation) during a 100-ps MD simulation in the canonical ensemble (NVT). A 100-ps MD simulation in the isobaric-isothermal ensemble (NPT) was carried out to equilibrate the system in constant pressure. The density was stabilized around 1.02 g/cm^3 during equilibration phase in constant pressure. Temperature and pressure were controlled by applying a weak coupling method (Berendsen *et al*., 1984), with temperature and pressure relaxation times τ_T = 1.0-ps and τ_p = 1.0-ps, respectively. MD simulations were performed in the NPT ensemble for 2-ns during production phase. Time step of 2-fs was used for all simulations and X-H bonds were constrained using the SHAKE algorithm (Ryckaert *et al*., 1977). Translational center of the mass motions was removed every1000 steps and coordinates were saved every 0.4-ps for analysis.

Analysis procedures: The Ptraj module of AMBER was used to extract root-mean-square deviations (RMSD) and root-mean-square fluctuations (RMSF) data from trajectories. RMSD is one of the most frequently used measures to investigate the structural changes of a protein, as follows:

$$RMSD = \sqrt{\frac{1}{N}\sum (r_i^{exp.} - r_i^{gen.})^2}$$

where $r_i^{exp.}$ and $r_i^{gen.}$ denote the Cartesian coordinates for atom *i* in the experimental and generated structures, respectively.

The dynamical properties of Cα atoms have been reported to contain sufficient information to investigate the most important motions in proteins (Amadei *et al*., 1993). Therefore, RMSF of Cα atoms was used to investigate structural flexibility, as follows:

$$RMSF = \sqrt{\frac{1}{N}\sum (r_i^{gen.} - r_i^{ave.})^2}$$

where $r_i^{gen.}$ denotes the Cartesian coordinates for atom *i* and $r_i^{ave.}$ denotes the time-averaged position for atom *i* in the trajectory.

Prior to calculating the RMSF, we removed the overall translational and rotational motions by superimposing backbone of each snapshot structure onto the one in the starting structure of the trajectory, using the least-squares fitting method.

RESULTS

Structural modeling and molecular docking analysis: A 3-D structural model of artemin was constructed based on ferritin structure and refined using MD simulation. To achieve a reliable structure, the final structural model passed two kinds of verification test: PSQS and Verify 3D which mainly focus on the local environment and ERRAT and ProCheck which mainly focus on local geometry (Table 1). Furthermore, based on the assignment of secondary structure, artemin contained 30% α-helix and 68% random coil which was in a good agreement with the previous experimental results reported by Rasti *et al*. (30.9% α-helix and 69.1% random coil).

As the experimental evidence proposes an RNA-binding ability for artemin at high temperatures *in-vivo*, we set a docking procedure for artemin and a RNA molecule. A short-length RNA was selected in order to reduce the structural effects of RNA molecule on the construction of complex and search for all possible RNA-binding sites in the structure of artemin. Docked molecular complexes were constructed and RNA binding sites were analyzed for the top 100 energy-ranked models. To identify binding sites, amino acid sequence of artemin was divided into five-residue windows and the binding energy between each window and RNA molecule was calculated for docked structures. The average of binding energy was calculated for each set of corresponding windows in all complexes. The cutoffs of < -10 Kcal/mol and < 7 A^o were considered for binding energy and protein-RNA distance respectively. Based on these cutoffs, six regions were considered as potent RNA-binding sites (Fig. 1A and 1B).

Artemin-RNA interaction sites: Further analyses with regards to frequency of binding sites-RNA interaction, average and standard deviation of binding energy in docked complexes revealed that windows 6 (His26-Pro30), 7 (Glu31-Ala35) and 37 (Trp181-Arg185) with the frequency of 100% for binding sites-RNA interaction, highly negative binding energy and low energy standard deviation can be considered as main RNA-binding sites in artemin (Table 2).

Amino acid sequence of these high potent sites were aligned and compared to other well-known RNA-binding sequences in order to find possible similar patterns. Alignment analyses revealed some similarities with regards to the type of interaction between RNA-binding sites of artemin with the specific class of RNA-binding proteins called PUFs (Fig. 2).

Molecular dynamics simulation: A docked structure with the most suitable condition revealing the binding energy of RNA-binding sites of artemin was selected for molecular dynamics simulation study to check the reliability of RNA-binding sites of artemin at 300 and 343 K. The stability of simulations was checked using the analysis of total energy changes during 100-ps

Tabel 1. Quality scores of artemin model with quality control programs.

Structure	Verify 3D	PSQS	ERRAT	ProCheck
Model of artemin	93.6	-0.33	92.2	91.5
Template (2fg4)	96.5	-0.36	99.3	94.1
Template (1aew)	87.7	-0.37	96.2	94.2

Data accessed from http://nihserver.mbi.ucla.edu/SAVS and http://www1.jcsg.org/psqs/psqs.cgi.

Table 2. Binding frequency and average of interaction energy for potent RNA-binding sites in top 100 energy-ranked docked models.

Window No.	Binding Frequency (%)	Average of interaction energy[a]	STDV[b]
5	40%	-17	20
6	100%	-52	4
7	100%	-47	17
21	80%	-14	13
33	72%	-15	30
37	100%	-60	2

a: unit of energy is Kcal/mol b: standard deviation of energy

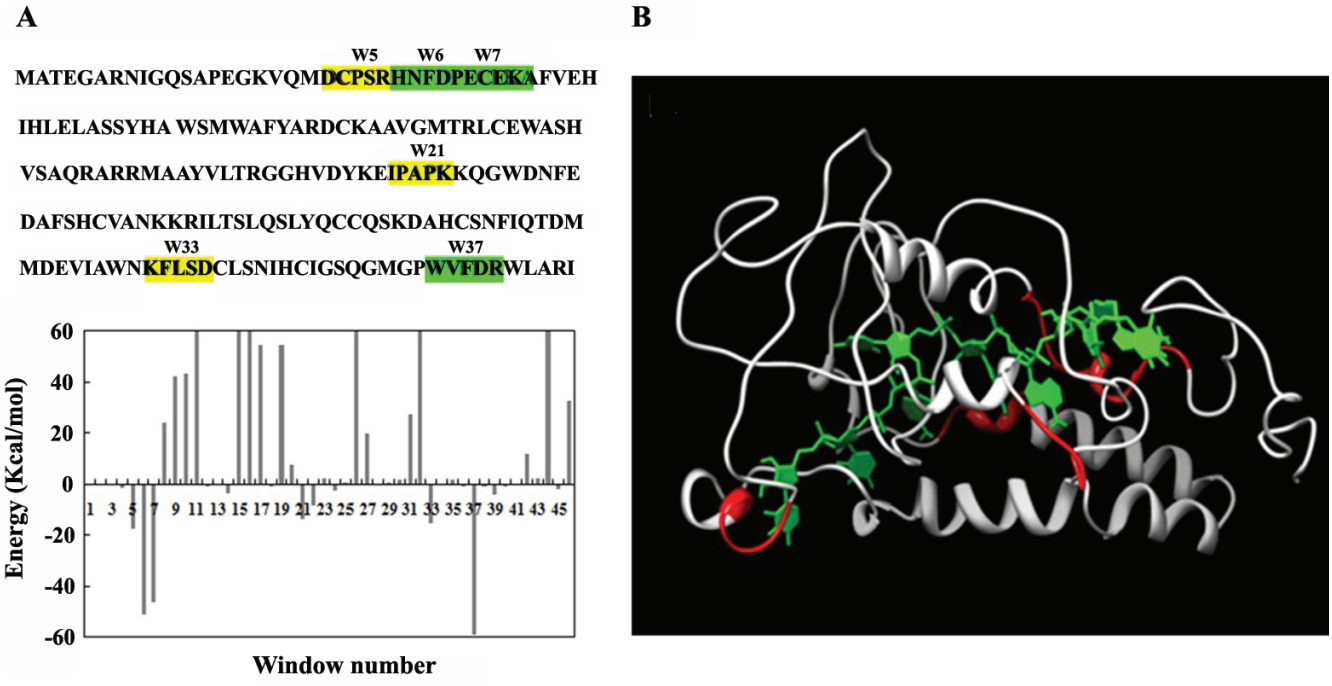

Figure 1. A: Artemin sequence. Potent RNA-binding sites are colored. Windows colored in green indicate the RNA-binging sites with the high potential for binding RNAs. The chart demonstrates average of binding energies between five-residue windows of artemin and RNA molecule for top 100 complexes. B: The ribbon view of artemin-RNA complex, showing that RNA-binding sites of artemin, colored in red, leads RNA molecule into the interior of artemin.

Protein	Conserved positions	
Pumilio	HGSRFI QLKLE	
	FGNYVI QKFFE	
	YGCRVI QKALE	
	NGNHVVQKCIE	
	YGCRVI QRILE	
	YGNYVI QHVLE	
	FASNVVEKCVT	
	YANYVVQKMID	
PUF-5	TGVKFLERHFP	
	AGNF I I QKFVE	
	FACRVVQMSIQ	
	CAI HVLQKVVK	
	YGCRLVQQTID	
	FANYVVQYVIK	
	YASHVVEGAFL	
	YGNYVVQQMIS	
PUF-6/7	SGVRFL EANYP	
	NGNF IV QKLVE	
	FACRVVQLALQ	
	IS I HVIQRVVK	
	YGCRLVQQVID	
	FANYVI QYVIK	
	YASH VI EGAFL	
	YGNYVVQQMIS	
Artemia	RHNF DPECEKA	residues 25 to 35
	MGPWVFDRWLA	residues 178 to 188

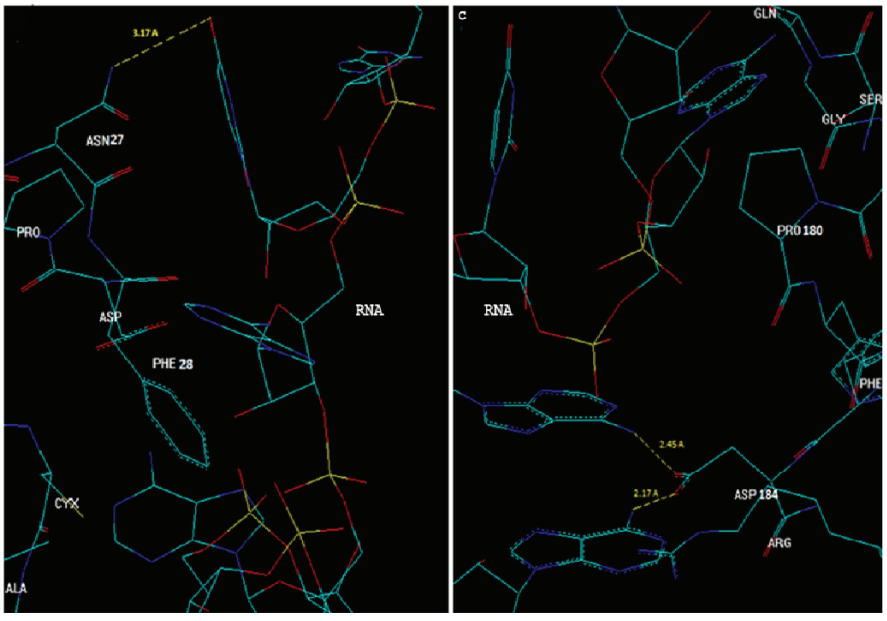

Figure 2. A: Sequence comparison of RNA-binding sites between artemin and PUF proteins. Conserved positions that are capable of making Van der Waals/H-bond, stacking and H-bond interactions with RNA molecules are colored in green, purple and red respectively. Following proteins were used for alignment: Pumilio from Homo sapiens (human) (NCBI accession number: NP_001018494), PUF-5 (NCBI accession number: NP_495814), PUF-6 (NCBI accession number: NP_496773) and PUF-7 (NCBI accession number: NP_500820) from *Caenorhabditis elegans*, and artemin from Artemia urmiana (NCBI accession number: ABY86224). Note: the sequence alignment between RNA-binding sites of PUF proteins refers to a previous investigation performed by Craig R. Stumpf *et al.* (2008) on PUF proteins. B: and C are Schematic representations of Van der Waals (Pro180), satck (Phe28) and H-bond (Asn27 and Asp184) interactions made between RNA-binding sites of aretmin and RNA molecule. The structures are shown by Chimera software.

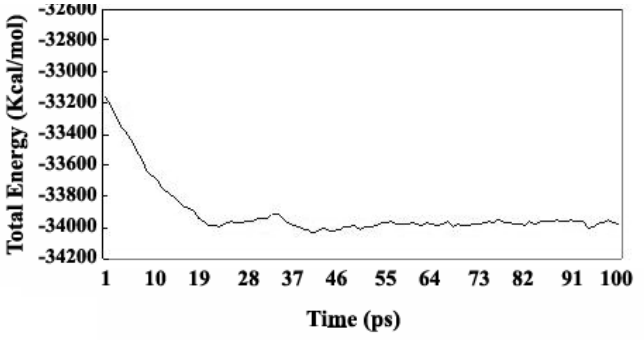

Figure 3. Total energy changes during 100-ps equilibration in constant pressure for artemin-RNA complex. The system was equilibrated and showed stable behavior after nearly 20-ps for simulations at 300 and 343 K.

equilibration at constant pressure as function of time. The system was equilibrated and showed stable behavior after nearly 20-ps for both simulations. The kinetic and potential energy changes in this equilibration phase also showed stable behavior in the simulations (Fig. 3). Temperature and density also became stabilized around 300 K (343 K for high temperature simulation) and 1.02 g/cm^3 respectively.

After MD simulation, binding energy was calculated between potent RNA-binding sites of artemin and RNA molecule, in the selected structure. For both simulations, the binding energy observed for each RNA-binding site was in a good agreement with the average of binding energy calculated (considering the standard deviations) for each set of correspondent sites in the top 100 energy-ranked models (Fig. 4). These outcomes can confirm the reliability of RNA-binding sites of artemin, showing that RNA keeps its location during the time of simulation. Models before and after MD were superimposed for a better comparison of structures and binding sites (Fig. 5). A RMSD of 1.23 was observed, showing the stability of complex at high temperatures.

Structural changes and motions: Comparison of RMSD between the structures of artemin and artemin-RNA complex revealed that the presence of RNA molecule and its interaction with artemin causes significant changes in the structure of artemin (Fig. 6A). Furthermore, the assignment of secondary structures revealed that compared to artemin, secondary structure content of artemin-RNA structure declined mostly due to the lack of two helical regions (Glu72-Ala79 and Phe112-His118), justifying their RMSD difference (data are not shown). Comparison of internal motions in artemin with those of artemin-RNA complex showed that firstly, there was a total decline in the RMSF of artemin-RNA structure compared to artemin structure; secondly, RNA-binding sites were mostly present in the low flexible regions (Fig. 6B).

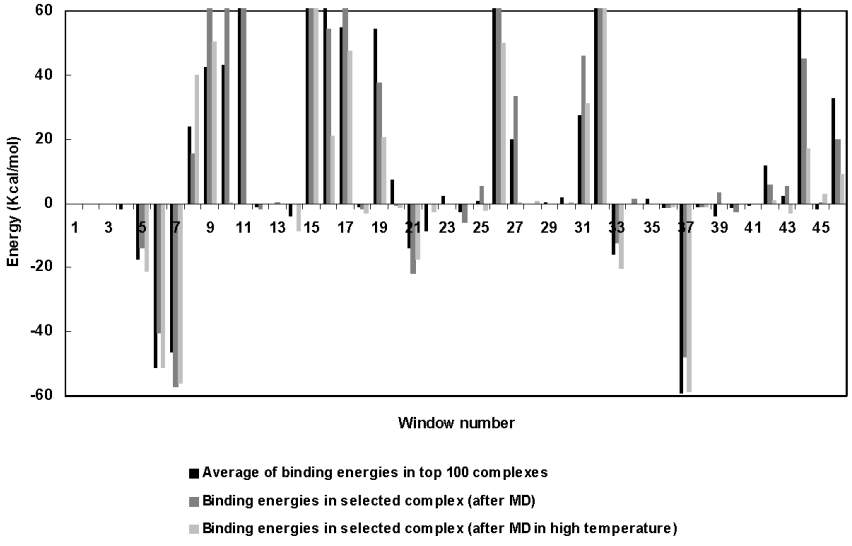

Figure 4. Comparison of binding energy between five-residue windows of artemin and RNA molecule in selected complex (after MD simulations at 300 and 343 K) with the average of binding energies between five-residue windows of artemin and RNA molecule in top 100 complexes.

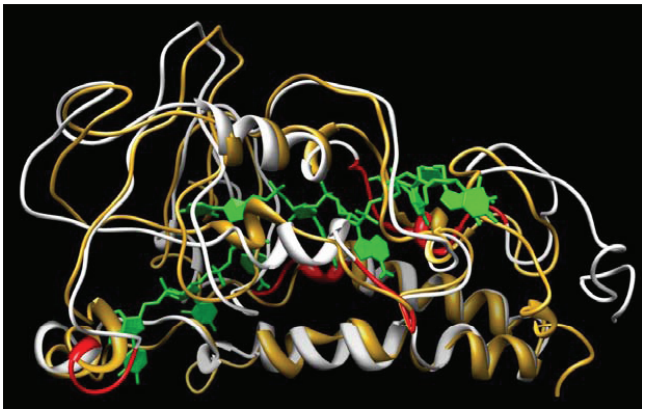

Figure 5. Superimposed view for complex structures before (white color) and after MD (golden color). Comparison of complexes shows no significant difference in secondary structure content and the situation of RNA-binding sites (red color).

DISCUSSION

As *Artemia* enters diapause stage, artemin appears in the cysts and soon after termination of harsh conditions and turning of cysts into larva, it disappears. It is known that processes such as DNA replication, transcription, translation, mitosis, cytokinesis and cell-division are substantially suppressed under the diapause condition. The presence of artemin in the period of diapause and its high tendency for binding RNAs suggests an RNA-protecting role for it. Based on this background, the present work has focused on the RNA-binding ability of artemin, using computational models, to investigate its probable RNA-binding role. Constructed model of artemin passed all kinds of verification tests, confirming its reliability for docking analysis. The most favorable docked structures, with regards to the binding energies, were selected to search for the potent RNA-binding sites in the structure of artemin. Analysis of binding energies identified two sites (His26-Ala35 and Trp181-Arg185) in the structure of artemin with high potential for binding RNAs. Alignment analyses showed that these binding sites in artemin and their corresponding RNA-binding sites in a specific class of RNA-binding proteins called PUFs show similar potential for binding RNAs with regards to the type of interactions (Fig. 2A). The main function of PUFs is regulation of various aspects of development by controlling mRNA stability which is similar to the suggested RNA-protecting role for artemin. It has been previously reported by Craig R. Stumpf *et al*. that the main interactions between PUF proteins and mRNAs are formed through amino acid residues that are located in 3 conserved positions, colored in Fig. 2A, in PUF repeats (Stumpf *et al*., 2008). These conserved positions are responsible for making Van der Waals/H-bond interactions (colored in green), stacking (colored in purple) and H-bond interactions (colored in red) with RNA molecules, respectively (Stumpf *et al*., 2008; Wang *et al*., 2002). In PUF proteins, residues such as Asn, Cys, Ser, Ile and Val, capable of making either H-bond or Van der Waals interactions, are present in the first conserved position. Similarly in artemin, this position is occupied by residues that are

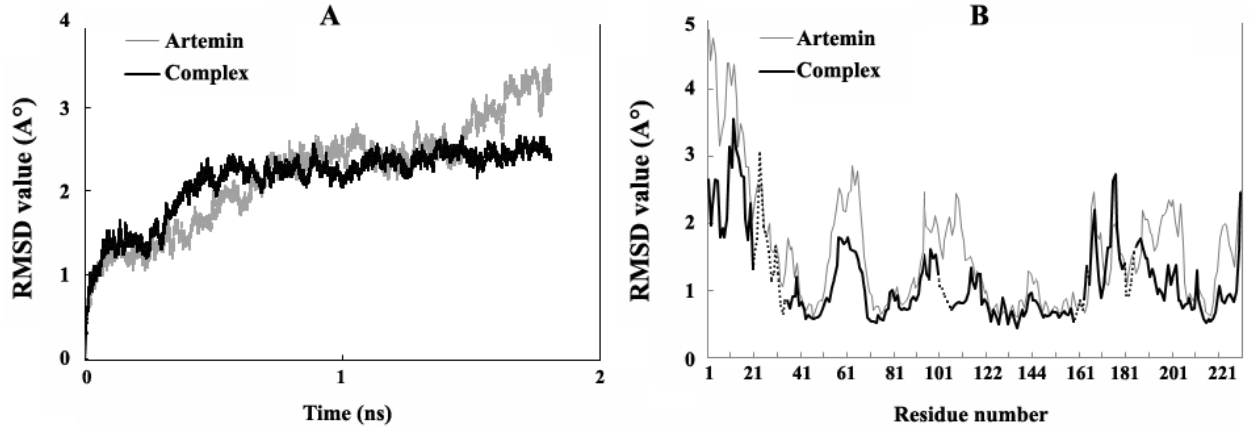

Figure 6. A: RMSD values of the structures in the trajectories over simulation time with respect to the first structure in artemin-RNA complex (black line) compared to artemin (gray line). B: Atomic positional fluctuations of Cα atoms in artemin-RNA complex (thick line) compared to artemin (thin line). RNA-binding sites are shown in dotted line.

able to make the similar types of interactions (Asn27 and Pro180) (Fig. 2B, C). The second conserved position in PUFs is mostly occupied by His, Phe, and Tyr residues, all capable of making stacking interaction. Phe28 and Trp181 with the ability of making the similar type of interactions are present in the corresponding position in artemin (Fig. 2B, C). Third conserved position in PUF proteins that is responsible for making hydrogen bonds with RNAs is placed by Glu and Gln. This position in RNA-binding sites of artemin contains Glu31 and Asp184 residues, both capable of making hydrogen bonds (Fig. 2B, C). Based on these results, it is suggested that the correspondent protein-RNA interacting positions in artemin and PUFs show similar potential for binding RNAs.

MD simulation studies at 300 and 343 K confirmed the location of two high potential RNA-binding sites in artemin (Fig. 4). Analysis of structural changes and motions showed that a significant decrease occurred in the secondary structure content and total RMSF of artemin in its complex state. Furthermore, it was shown that RNA-binding sites are mostly present in the low flexible regions (mainly the core of the protein) in such a way that leads RNA molecule into the interior of the protein (Fig. 1B). Regarding the homology found between artemin and ferritins, it seems that artemin's cavity is correspondent to the Fe-binding cavity in ferritins and let different parts of RNA to penetrate into the interior of the protein. Finally, findings of the present study can strengthen the previous reports that suggested an RNA-protecting role for artemin in the diapause state.

Acknowledgments

This work was financially supported by the research council of the University of Guilan. We express our gratitude to the Modeling Center of the Tarbiat Modarres University for supporting us with AMBER 9 program, Mr. M. Rassa and Miss. M. Molakarimi for their help.

References

Aloy P, Moont G, Gab HA, Querol E, Aviles FX, Sternberg MJE (1998). Modelling repressor proteins docking to DNA. *Proteins*. 33: 535-549.

Amadei A, Linssen AB, Berendsen HJ (1993). Essential dynamics of proteins. *Proteins*. 17: 412-425.

Berendsen HJC, Postma JPM, Van Gunsteren WF, Dinola A, Haak JR (1984). Molecular dynamics with coupling to an external bath. *J Chem Phys*. 81: 3684-3690.

Berman HM, Olson WK, Beveridge DL, Westbrook J, Gelbin A, Demeny T, Hsieh SH, Srinivasan AR, Schneider B (1992). The Nucleic Acid Database - a comprehensive relational database of three-dimensional structures of nucleic acids. *Biophys J*. 63: 751-759.

Bowie JU, Lüthy R, Eisenberg D (1991). A method to identify protein sequences that fold into a known three-dimensional structure. *Science*. 12: 164-170.

Case DA, Darden TA, Cheatham TE, Simmerling CL, Wang J, Duke RE, Luo R, Merz KM, Wang B, Pearlman DA, Crowley M, Brozell S, Tsui V, Gohlke H, Mongan J, Hornak V, Cui G, Beroza P, Schafmeister C, Caldwell JW, Ross WS, Kollman PA (2006). *AMBER 9*. University of California, San Francisco.

Chen T, Amons R, Clegg JS, Warner AH, MacRae TH (2003). Molecular characterization of artemin and ferritin from *Artemia franciscana*. *Eur J Biochem*. 270: 137-145.

Chen T, Villeneuve TS, Garant KA, Amons R, MacRae TH (2007). Functional characterization of artemin, a ferritin homolog synthesized in *Artemia* embryos during encystment and diapauses. *FEBS J.* 274: 1093-1101.

Colovos C, Yeates TO (1993). Verification of protein structures: patterns of nonbonded atomic interactions. *Protein Sci*. 2: 1511-1519.

Curtis D, Lehmann R, Zamore PD (1995). Translational regulation in development. *Cell* 81: 171-178.

Gabb HA, Jackson RM, Sternberg MJE (1997). Modelling protein docking using shape complementarity, electrostatics and biochemical information. *J Mol Biol*. 272: 106-120.

Godzik A (1996). Knowledge-based potentials for protein folding: what can we learn from known protein structures? *Structure*. 4: 363-366.

Godzik A, Kolinski A, Skolnick J (1995). Are proteins ideal mixtures of amino acids? Analysis of energy parameter sets. *Protein Sci*. 4: 2107-2117.

Heinig M, Frishman D (2004). STRIDE: a Web server for secondary structure assignment from known atomic coordinates of proteins. *Nucleic Acids Res*. 32: 500-502.

Hempstead PD, Yewdall SJ, Fernie AR, Lawson DM, Artymiuk PJ, Rice DW, Ford GC, Harrison PM (1997). Comparison of the three-dimensional structures of recombinant human H and horse L ferritins at high resolution. *J Mol Biol*. 268: 424-448.

Hontoria F, Crowe JH, Crowe LM, Amat F (1993). Metabolic heat production by *Artemia* embryos under anoxic conditions. *J Exp Biol*. 178: 149-159.

Jaroszewski L, Pawlowski K, Godzik A (1998). Multiple Model Approach: Exploring the limits of comparative modeling. *J Mol Model*. 4: 294-309.

Johnstone O, Lasko P (2001). Translational regulation and RNA localization in Drosophila oocytes and embryos. *Annu Rev Genet*. 35: 365-406.

Jorgensen WL, Chandrasekhar J, Madura J, Klein ML (1983). Comparison of simple potential functions for simulating liquid water. *J Chem Phys*. 79: 926-935.

Laskowski RA, MacArthur MW, Moss DS, Thornton JM (1993). PROCHECK - a program to check the stereochemical quality of protein structures. *J App Cryst*. 26: 283-291.

MacRae TH (2003). Molecular chaperones, stress resistance and development in *Artemia franciscana*. *Semin Cell Dev Biol*.

14: 251-258.

Pawlowski K, Jaroszewski L, Bierzynski A, Godzik A (1997). Multiple model approach-dealing with alignment ambiguities in protein modeling. *Pac Symp Biocomput*. 4: 328-339.

Rasti B, Shahangian SS, Sajedi RH, Taghdir M, Hasannia S, Ranjbar B (2009). Sequence and structural analysis of artemin based on ferritin: A comparative study. *Biochim Biophys Acta*. 1794: 1407-1413.

Ryckaert JP, Ciccotti G, Berendsen HJC (1977). Numerical integration of the cartesian equations of motion of a system with constraints: molecular dynamics of n-alkanes. *J Comput Phys*. 23: 327-341.

Sali A, Blundell TL (1993). Comparative protein modeling by satisfaction of spatial restraints. *J Mol Biol.* 234: 779-815.

Stumpf CR, Kimble J, Wickens M (2008). A *Caenorhabditis elegans* PUF protein family with distinct RNA binding specificity. *RNA*. 14: 1550-1557.

Thompson JD, Higgins DG, Gibson TJ (1994). Clustal w: improving the sensitivity of progressive multiple sequence alignment through sequence weighting, position specific gap penalties and weight matrix choice. *Nucleic Acids Res*. 22: 4673-4680.

Wang X, McLachlan J, Zamore PD, Hall TMT (2002). Modular Recognition of RNA by a Human Pumilio-Homology Domain. *Cell*. 110: 501-512.

Wang Z, Li C, Ellenburg M, Soistman E, Ruble J, Wright B, Ho JX, Carter DC (2006). Structure of human ferritin L chain. *Acta Crystallogr D Biol Crystallogr*. 7: 800-806.

Warner AH, Brunet RT, MacRae TH, Clegg JS (2004). Artemin is an RNA-binding protein with high thermal stability and potential RNA chaperone activity. *Arch Biochem Biophys*. 424: 189-200.